



**POLITECNICO**  
**MILANO 1863**

**SCUOLA DI INGEGNERIA INDUSTRIALE  
E DELL'INFORMAZIONE**



## Title

**MSc in Space Engineering**

**Authors:**

10723712	MARCELLO PARESCHI	(BSc Aerospace Engineering - Politecnico di Milano)
10836125	DANIELE PATERNOSTER	(BSc Aerospace Engineering - Politecnico di Milano)
10711624	ALEX CRISTIAN TURCU	(BSc Aerospace Engineering - Politecnico di Milano)
10884250	TAMIM HARUN OR	(BSc Aerospace Engineering - International Islamic University Malaysia)

**Professor:** CAMILLA COLOMBO

**Academic year:** 2023-2024

---

## Abstract

Lorem ipsum dolor sit amet, consectetuer adipiscing elit. Ut purus elit, vestibulum ut, placerat ac, adipiscing vitae, felis. Curabitur dictum gravida mauris. Nam arcu libero, nonummy eget, consectetuer id, vulputate a, magna. Donec vehicula augue eu neque. Pellentesque habitant morbi tristique senectus et netus et malesuada fames ac turpis egestas. Mauris ut leo. Cras viverra metus rhoncus sem. Nulla et lectus vestibulum urna fringilla ultrices. Phasellus eu tellus sit amet tortor gravida placerat. Integer sapien est, iaculis in, pretium quis, viverra ac, nunc. Praesent eget sem vel leo ultrices bibendum. Aenean faucibus. Morbi dolor nulla, malesuada eu, pulvinar at, mollis ac, nulla. Curabitur auctor semper nulla. Donec varius orci eget risus. Duis nibh mi, congue eu, accumsan eleifend, sagittis quis, diam. Duis eget orci sit amet orci dignissim rutrum.

# Contents

<b>Abstract</b>	<b>1</b>
<b>Contents</b>	<b>2</b>
<b>1 Interplanetary mission</b>	<b>3</b>
1.1 Introduction . . . . .	3
1.1.1 Description of the problem . . . . .	3
1.1.2 Assigned data and constraints . . . . .	3
1.2 Algorithms description . . . . .	3
1.2.1 Brute force algorithm . . . . .	3
1.2.2 Gradient descent algorithm . . . . .	4
1.3 Reduction of the time windows . . . . .	4
1.3.1 Resonance period analysis . . . . .	4
1.3.2 Cost-plot analysis . . . . .	5
1.3.3 Final time window selection . . . . .	5
1.4 Conclusion and results . . . . .	5
<b>2 Planetary mission</b>	<b>6</b>
2.1 Introduction . . . . .	6
2.1.1 Nominal Orbit . . . . .	6
2.2 Groundtrack . . . . .	6
2.2.1 Unperturbed Groundtrack . . . . .	7
2.2.2 Perturbed Groundtrack . . . . .	8
2.3 Orbit Propagation . . . . .	9
2.3.1 History of the Keplerian Elements . . . . .	9
2.3.2 Representation of the Evolution of the Orbit . . . . .	11
2.3.3 Filtering . . . . .	11
2.4 Comparison with Real Data . . . . .	12
<b>Bibliography</b>	<b>12</b>

# 1. Interplanetary mission

## 1.1. Introduction

### 1.1.1. Description of the problem

The first part of the assignment aims at designing an interplanetary transfer from Mars to asteroid 1036 Ganymed exploiting a powered gravity assist on Earth. The problem is analyzed through the patched conics method, without considering the injection and arrival hyperbolae. The initial and final velocity vector of the satellite are assumed to be the same of the respective celestial body. The two heliocentric legs are calculated through the Lambert problem. The trajectory is selected with the only criteria of minimizing the cost of the mission, assessed through the total  $\Delta V$ . The latter is computed by summing different contributions:

$$\Delta V_{tot} = \Delta V_1 + \Delta V_2 + \Delta V_3 \quad (1.1)$$

where  $V_{-,i}$  and  $V_{+,i}$  are the velocity vectors before and after the  $i$ -th manoeuvre respectively.

Where the three terms are defined as:

- $\Delta V_1$  related to the injection in the first heliocentric leg;
- $\Delta V_2$  related to the exit from the second heliocentric leg;
- $\Delta V_3$  related to the impulse given by the engine at pericentre of hyperbola fly-by;

All the manoeuvres are assumed to be impulsive, i.e. they change only the velocity vector of the spacecraft, maintaining invariated the position vector. Note that  $\Delta V_1$  and  $\Delta V_2$  are related to heliocentric velocities, while  $\Delta V_3$  is calculated through relative geocentric velocities.

For each manoeuvre the cost is computed as:

$$\Delta V_i = \|V_{+,i} - V_{-,i}\| \quad (1.2)$$

### 1.1.2. Assigned data and constraints

A few constraints were considered:

- earliest departure date  $t_{min,dep} = [01/01/2028 00 : 00 : 00]$  in Gregorian calendar
- latest arrival date  $t_{max,arr} = [01/01/2058 00 : 00 : 00]$  in Gregorian calendar
- time of flights of the two heliocentric arcs must be greater than the associated parabolic time
- minimum pericentre radius of the fly-by hyperbola  $r_p = r_E + 500 \text{ km}$
- single-revolution Lambert problem was considered
- reasonable total time of the mission

Note that the constraint on the pericentre radius of the fly-by is considered both for avoid impact on Earth and to prevent undesired atmospheric drag effects.

## 1.2. Algorithms description

The targeting problem previously defined can be seen as an optimization problem with three degrees of freedom (DOFs). Indeed, once the departing date and the two times of flight of the heliocentric legs are chosen, both the Lambert's arcs and the fly-by hyperbola are fully defined. Regarding the formulation of the Lambert's problem, it requires the knowledge of the initial and final position and also the imposed time of flight between them. For two Lambert's arcs it would be needed a total of six DOFs, but this quantities are dependant one to each other:

- the final position vector of the first arc corresponds to the initial position of the second one;
- the initial date for the departing on the second arc corresponds the arrival date on the first arc;
- fixing the first Lambert's arc, the final position and arrival date for the second Lambert's arc are related through the analytical ephemerides.

Once the two heliocentric legs are determined, the powered gravity assist follows as the geocentric velocity vectors are known.

Two methods were implemented to solve the optimization problem: **brute force algorithm** and the **gradient descent algorithm**.

### 1.2.1. Brute force algorithm

---

**Algorithm 1** Bruteforce algorithm

---

```

Require:  $T_{dep}, T_{flyby}, T_{arr}$ 
Ensure:  $\Delta V_{min}$ 
 $\Delta V_{min} = 10^{10}$ 
for  $i$  in  $T_{dep}$  do
    for  $j$  in  $T_{flyby}$  do
        for  $k$  in  $T_{arr}$  do
            end for
        end for
    end for

```

---

### 1.2.2. Gradient descent algorithm

Algorithm 1

## 1.3. Reduction of the time windows

### 1.3.1. Resonance period analysis

The first natural reduction on the domain of interest that could come to mind is to search the frequency on which the three celestial bodies repeat the relative positions on their orbits. On the approximation of circular orbits, this particular time period would be the synodic period generalized for the case of three bodies. However, this path is unviable because the orbit of the asteroid has a relevant eccentricity. To better comprehend the problem of having that eccentricity, particular attention have to be paid on the definitions of phasing and synodic period for two bodies:

- **Phasing**  $\phi \rightarrow$  the angle between two celestial bodies, calculated as the difference in their **true anomalies**:

$$\phi(t) = \theta^{(2)}(t) - \theta^{(1)}(t) \quad (1.3)$$

- **Synodic period**  $T_{syn} \rightarrow$  if two celestial bodies have initial phasing  $\phi_0$ , they will return to the same phasing after a synodic period  $T_{syn}$ :

$$\phi(t_0) = \phi_0 \quad \rightarrow \quad \phi(t_0 + T_{syn}) = \phi_0 \quad (1.4)$$

As the definitions rely on the **true anomalies** of celestial bodies, non-circular orbits mean that the same phasing does NOT imply the same relative positions between them. In other words, once the synodic period has passed, the phasing of the three considered bodies keeps unchanged but it could result in a completely different relative positions with respect to the initial condition.

The problem needs to be reformulated. The goal is to find the period of time that elapses between a state of orbital positions of the bodies and the next occurrence of the same state. In literature, this particular period is called **period of orbital resonance** and it will be here indicated as  $T_{res}$ . Supposing that the orbits keep the other Keplerian elements unchanged during the revolution, the relation on true anomalies can be expressed as:

$$\begin{cases} \theta^{(1)}(t_0) = \theta_0^{(1)} \\ \theta^{(2)}(t_0) = \theta_0^{(2)} \\ \theta^{(3)}(t_0) = \theta_0^{(3)} \end{cases} \rightarrow \begin{cases} \theta^{(1)}(t_0 + T_{res}) = \theta_0^{(1)} \\ \theta^{(2)}(t_0 + T_{res}) = \theta_0^{(2)} \\ \theta^{(3)}(t_0 + T_{res}) = \theta_0^{(3)} \end{cases} \quad (1.5)$$

Since the true anomaly for an orbit repeats itself every orbital period  $T$ , it results:

$$\begin{cases} \theta_0^{(1)} = \theta^{(1)}(t_0 + iT^{(1)}) = \theta^{(1)}(t_0 + T_{res}) \\ \theta_0^{(2)} = \theta^{(2)}(t_0 + jT^{(2)}) = \theta^{(2)}(t_0 + T_{res}) \\ \theta_0^{(3)} = \theta^{(3)}(t_0 + kT^{(3)}) = \theta^{(3)}(t_0 + T_{res}) \end{cases} \rightarrow T_{res} = iT^{(1)} = jT^{(2)} = kT^{(3)} \quad (i, j, k \in \mathbb{N}) \quad (1.6)$$

As obtained in [Equation 1.6](#), the resonance period  $T_{res}$  must be a multiple of all the three orbital periods. To find

three compatible natural numbers for  $i, j, k$ , the following procedure can be followed:

```

 $i = 1; \quad j = i \cdot T^{(1)}/T^{(2)}; \quad k = i \cdot T^{(1)}/T^{(3)}$ 
while  $j \notin \mathbb{N}$  or  $k \notin \mathbb{N}$  do            $\triangleright$  a tolerance  $tol$  must be implemented
     $i = i + 1$ 
     $j = i \cdot T^{(1)}/T^{(2)}$ 
     $k = i \cdot T^{(1)}/T^{(3)}$ 
end while
return  $i, j, k$ 
```

Note that, since a perfect resonance of three celestial bodies is realistically impossible, a certain tolerance  $tol$  must be introduced when evaluating  $j, k \in \mathbb{N}$  in order to compute a reasonable  $T_{res}$ . In the specific case of this report, the execution of the above algorithm returned the following results:

$tol$	$i$ (Earth)	$j$ (Mars)	$k$ (1036 Ganymed)
0.1159	13	6.9119	4.8841

**Table 1.1:** Results of the resonance analysis

$T_{res}$  results to be 13 Earth's sidereal years, so the time domain can be restricted accordingly. It is important to keep in mind that this is an approximation, but since the mission has to depart in a reasonable date, it is acceptable to restrain the time window to the first 13 years. In any case, the cost of the mission will repeat similarly after 13 years.

### 1.3.2. Cost-plot analysis

### 1.3.3. Final time window selection

## 1.4. Conclusion and results

[1]

# 2. Planetary mission

## 2.1. Introduction

The PoliMi Space Agency wants to launch a Planetary Explorer Mission, to perform Earth Observation. This section carries out relevant orbital analysis and groundtrack estimation while also considering two perturbation models. A modified groundtrack was proposed for a repeating groundtrack, and two propagation methods are used to perform the analysis which are then compared. A comparison between the real data of a satellite and its analytical results obtained with the code model is also performed for model validity.

### 2.1.1. Nominal Orbit

From the provided orbital parameters this satellite heavily contains geosynchronous orbital characteristics. Hence, the altitude at perigee is chosen as 35786 km - where it is possible to see the moon and J2 perturbation effect.  $\Omega$  (right ascension of ascending node),  $\omega$  (argument of perigee), and  $f_0$  (initial true anomaly) are chosen arbitrarily for a simpler analysis.

a [km]	e [-]	i [°]	$\Omega$ [°]	$\omega$ [°]	altitude at perigee [km]
42159	0.0007	32.5934	0	85	35786

Table 2.1: Keplerian elements of the orbit

The unperturbed nominal orbit is propagated as below in the Earth-centered reference frame:

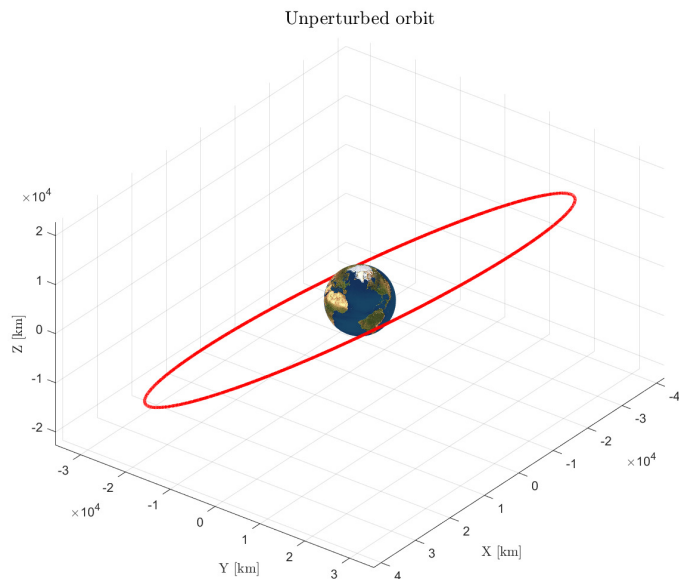


Figure 2.1: Assigned orbit

## 2.2. Groundtrack

The satellite's orbit is propagated to compute its groundtrack. The motion of the spacecraft is assumed to be a perturbed two body problem in Cartesian coordinates, described by the equation:

$$\dot{\mathbf{r}} = -\frac{\mu}{r^3} \mathbf{r} + \mathbf{a}_{\text{perturbation}} \quad (2.1)$$

This is solved using MATLAB's multi-step solver `ode113` function which is based on the Adams-Bashforth-Moulton method; it's chosen for its high accuracy over an extended period. A relative tolerance of  $1 \times 10^{-12}$  and absolute tolerance of  $1 \times 10^{-12}$  were selected for more precision.

### 2.2.1. Unperturbed Groundtrack

#### Nominal Orbit Groundtrack

The first required analysis of the ground track is for the nominal orbit considering an unperturbed case, where the  $\mathbf{a}_{\text{perturbation}}$  in equation is null. The ground track was propagated for a period of 1 orbit of the satellite, 1 day and 10 days, as shown below.

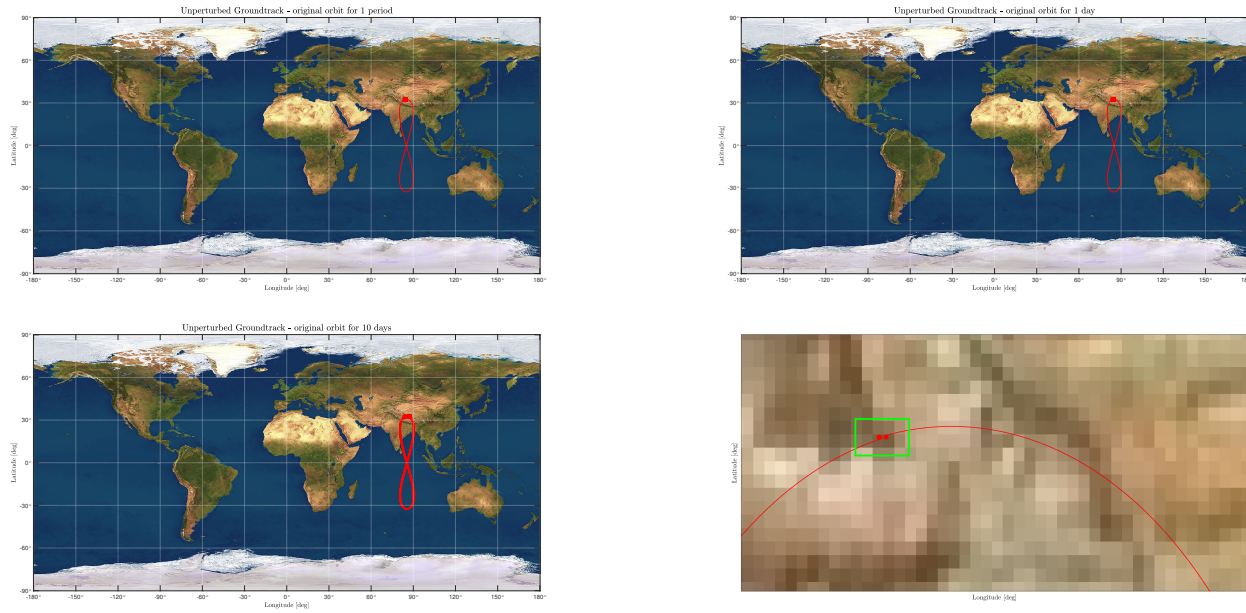


Figure 2.2: Ground track of the unperturbed nominal orbit during: (a) 1 orbit; (b) 1 day; (c) 10 days. Ground track path (—), Starting point (●), Ending point (■).

The groundtrack of this satellite has formed an “8” shape, a phenomenon known as the figure-eight groundtrack. At geosynchronous altitude, the location after one revolution is the same, and for geostationary orbits, the satellite always appears to be stationary over one location. The figure “8” occurs because the satellites relative velocity is less and greater, than locations on the Earth as it travels from the ascending node.

#### Repeating Groundtrack

For establishing a good communication with the network of ground stations of PoliMi Space Agency, a repeating ground track with a ratio of 1:1 (for each orbit of the spacecraft, Earth has performed 1 revolution) is maintained. Therefore, the period of the repeating ground track orbit is computed. For an unperturbed orbit, the period is only a function of the semi-major axis and can be calculated to get the desired repeating ground track. Both equations are listed below. By extension, the other orbital parameters are kept the same as the nominal orbit.

$$T_{\text{repeating}} = \frac{1}{1} T_{\text{Earth}} \quad T = 2\pi \sqrt{\frac{a^3}{\mu}} \rightarrow a_{\text{repeating}} = 42166 \text{ km} \quad (2.2)$$

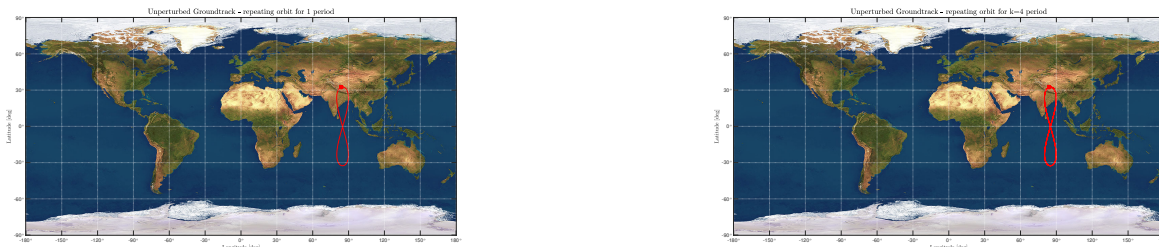


Figure 2.3: Ground track of the unperturbed repeating orbit during: (a) 1 orbit; (b) 4-k=4 orbits. Ground track path (—), Starting point (●), Ending point (■).

## 2.2.2. Perturbed Groundtrack

### Assigned Perturbations

This project has been assigned with two perturbations:  $J_2$  effect and Moon perturbation.  $J_2$  effect consists of a perturbing potential on top of the central gravity field of the Earth. In order to model it, a zonal harmonic potential is used, function of the geocentric distance  $r$  and of the coelevation  $\phi$ .

$$R(r, \phi) = \frac{\mu}{r} \left( -1 + \sum_{n=2}^{\infty} \left( \frac{R_E}{r} \right)^n J_n P_n(\cos \phi) \right) \quad (2.3)$$

Here,  $J_2$  term is considered for modelling which is correlated to Earth oblateness. The perturbing acceleration due to  $J_2$  effect is given as:

$$\mathbf{a}_{J_2} = \frac{3 J_2 \mu R_E^2}{2 r^4} \left[ \left( \frac{x}{r} \left( \frac{5z^2}{r^2} - 1 \right) \right) \mathbf{i} + \left( \frac{y}{r} \left( \frac{5z^2}{r^2} - 1 \right) \right) \mathbf{j} + \left( \frac{z}{r} \left( \frac{5z^2}{r^2} - 3 \right) \right) \mathbf{k} \right] \quad (2.4)$$

Perturbation due to the moon acting on the orbit is modelled through a two body problem scenario taking into account the force of the moon as a perturbing acceleration. This acceleration is computed from:

$$\mathbf{a}_{\text{Moon}} = \mu_{\text{Moon}} \left( \frac{\mathbf{r}_{m/s}}{r_{m/s}^3} - \frac{\mathbf{r}_m}{r_m^3} \right) \quad (2.5)$$

where  $\mathbf{r}_{m/s}$  is the vector that goes from the S/C to the moon and  $\mathbf{r}_m$  is the vector that goes from Earth to Moon.

Possible perturbations are charted in autoreffig:orbit perturbations. It is observed that the  $J_2$  effect ( $C_{2,0}$  in figure) and moon perturbation are one of the primary sources of orbital perturbation. Hence, our models and altitude choice are consistent.

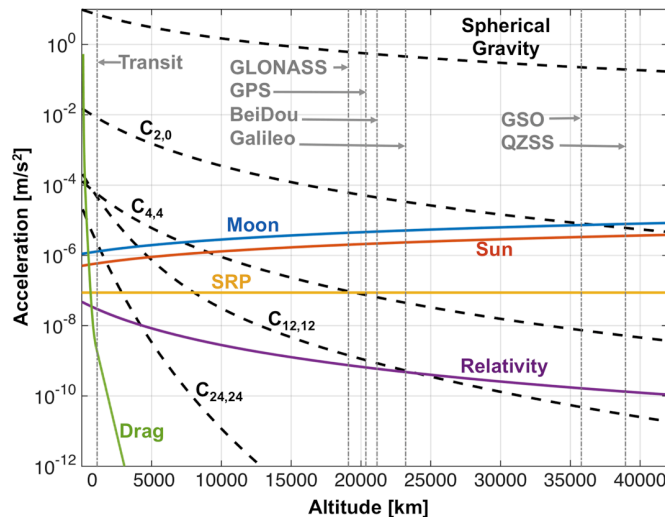
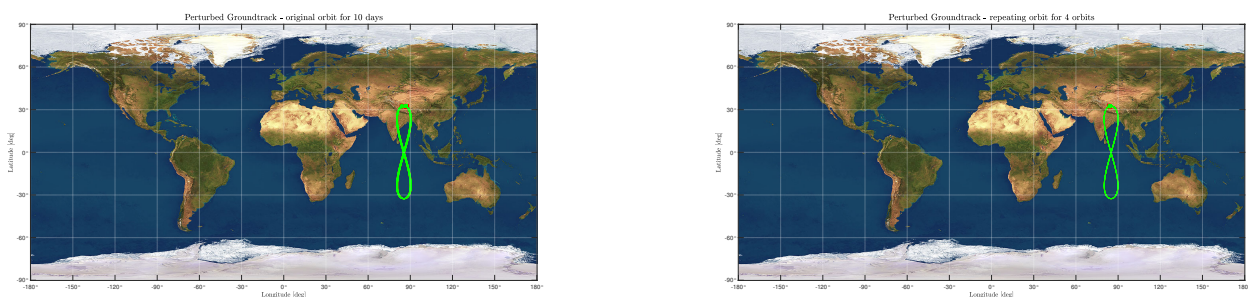
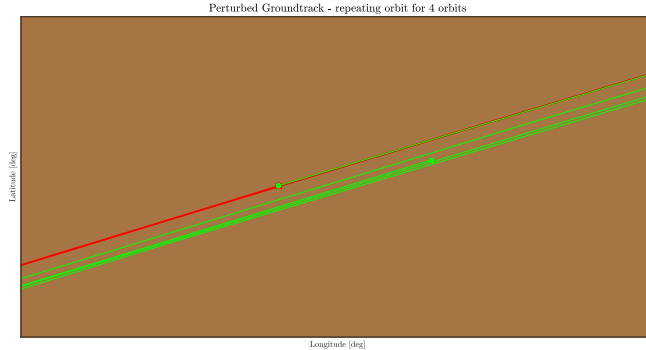


Figure 2.4: Orbit Perturbations

### Nominal and Repeating Groundtrack





**Figure 2.5:** Ground track of the perturbed orbits: (a) Nominal orbit during 10 days; (b) Repeating orbit during 4 orbits; (c) Perturbation effect for repeating orbit. Ground track of unperturbed (—), Starting point (●), Ending point (■); Ground track of perturbed (—), Starting point (●), Ending point (■).

It is observed that the perturbations have a great impact on the ground track path of the satellite. Both the nominal and repeating orbits get out of phase with relation to the unperturbed case. From Figure 2.5, the repeating ground track orbit proposed does not work in the presence of assigned perturbations.

## 2.3. Orbit Propagation

Orbits were propagated using Cartesian coordinates (Newton's equations of motion), or Keplerian elements (Gauss' planetary equations). Gauss' equations are presented in the Radial-Transversal-Out-of-plane reference frame (RSW). All formulas can be found in (CITE CURTIS HERE!).

$$\begin{aligned}
 \frac{da}{dt} &= \frac{2a^2}{h} \left( e \sin f a_r + \frac{p}{r} a_s \right) \\
 \frac{de}{dt} &= \frac{1}{h} (p \sin f a_r + ((p+r) \cos f + r e) a_s) \\
 \frac{di}{dt} &= \frac{r \cos(f+\omega)}{h} a_w \\
 \frac{d\Omega}{dt} &= \frac{r \sin(f+\omega)}{h \sin i} a_w \\
 \frac{d\omega}{dt} &= \frac{1}{h e} (-p \cos f a_r + (p+r) \sin f a_s) - \frac{r \sin(f+\omega) \cos i}{h \sin i} a_w \\
 \frac{df}{dt} &= \frac{h}{r^2} + \frac{1}{e h} (p \cos f a_r - (p+r) \sin f a_s)
 \end{aligned} \tag{2.6}$$

For the moon perturbation, which cannot be directly expressed in RSW frame, it's possible to transform the perturbing accelerations from Cartesian to RSW. The three rotation matrices for this are shown below where a rotation of  $\Omega$  around the third axis of the inertial frame is performed, then a rotation of  $i$  around the first axis of the rotated frame, and finally a rotation of an angle  $\theta + \omega$  around the third axis of the last frame.

$$R_\Omega = \begin{bmatrix} \cos \Omega & \sin \Omega & 0 \\ -\sin \Omega & \cos \Omega & 0 \\ 0 & 0 & 1 \end{bmatrix}; \quad R_i = \begin{bmatrix} 1 & 0 & 0 \\ 0 & \cos i & \sin i \\ 0 & -\sin i & \cos i \end{bmatrix}; \quad R_{\theta+\omega} = \begin{bmatrix} \cos(\theta+\omega) & \sin(\theta+\omega) & 0 \\ -\sin(\theta+\omega) & \cos(\theta+\omega) & 0 \\ 0 & 0 & 1 \end{bmatrix} \tag{2.7}$$

### 2.3.1. History of the Keplerian Elements

The Keplerian elements were obtained through the integration of the equation of motion and of the Gauss planetary equations. The propagation time is taken as 10 years, so it's sufficient to see the perturbations properly developed for this project's case. The evolution of the data and of the relative error between both methods of integration are presented below:

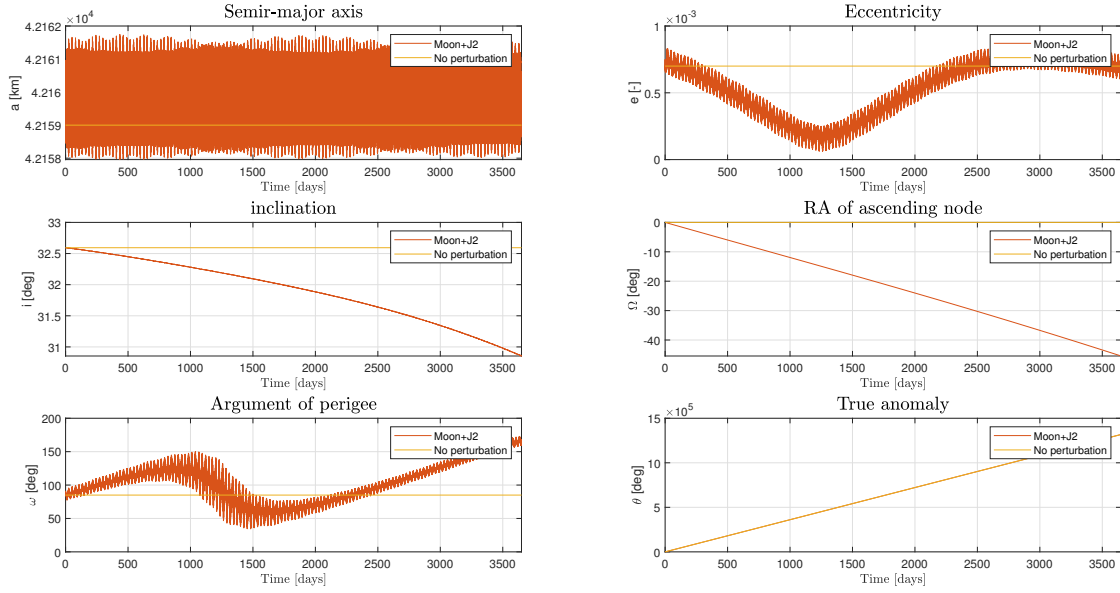


Figure 2.6: Evolution of the data

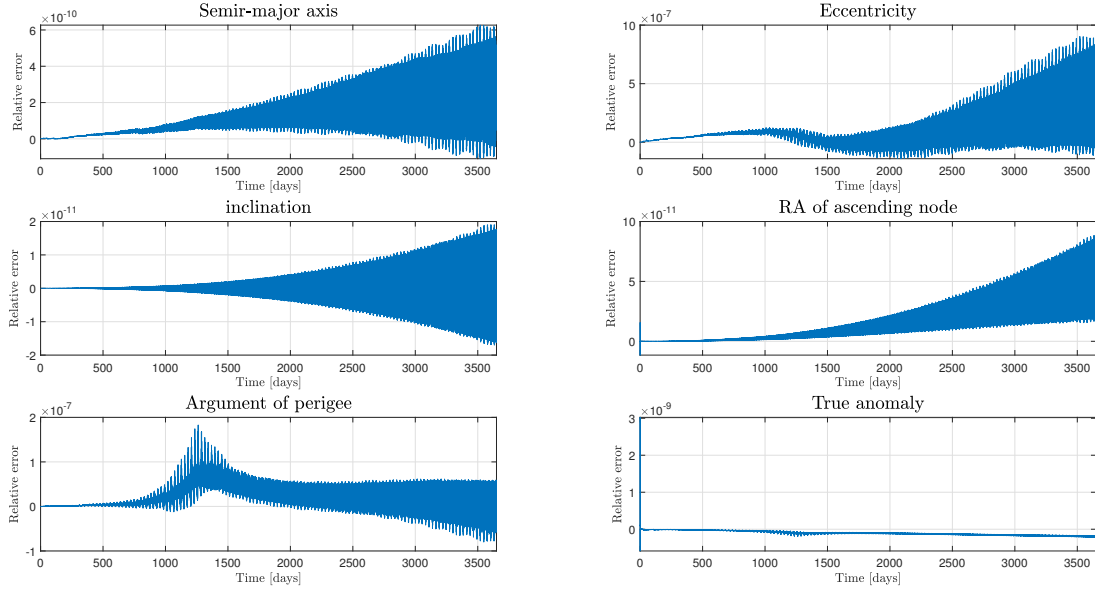


Figure 2.7: Relative error between both methods of integration

It is possible to distinguish a long-periodic behaviour and a short-periodic behaviour by looking at the evolution of orbital elements. It is very clear for eccentricity  $e$ , inclination  $i$ , and also for argument of perigee  $\omega$  to a sufficient extent. Semi-major axis presents both short-periodic and long-periodic behaviour. As for the right ascension of ascending node  $\Omega$ , and true anomaly  $f$ , the short-periodic behaviour is less visible but still present. From Figure 2.7 of relative error between Gauss' resolution and Cartesian resolution, it can be observed that the two methods are equivalent if the precision of the two is compared.

### 2.3.2. Representation of the Evolution of the Orbit



Figure 2.8: Orbit evolution representation in the 3D plane. Colors are used in order to let the reader understand the evolution of the orbit: in chronological order there are (—), (—), (—), (—), (—), (—), (—), and (—). The initial position of spacecraft is (\*) and the final position of spacecraft is (\*).

### 2.3.3. Filtering

The filtering of results is now performed to see how the perturbations generate behaviours with different frequencies, and to retrieve the long-period and the secular evolution of the data.

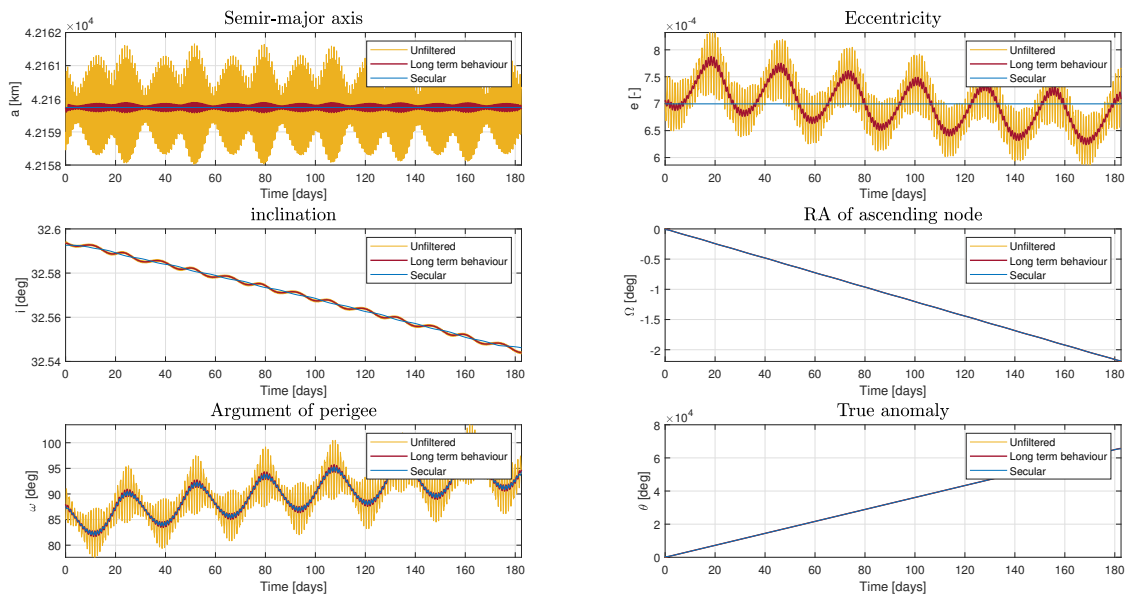


Figure 2.9: Orbit Perturbations

Here, long-periodic behaviour is related to moon perturbation and short-periodic perturbation is related to J2 effect. This is due to the fact that the J2 perturbation is related to the oblateness of the Earth and of the S/C's orbit, whose period is much lower than the Moon orbit period. Two different filters are used: the filter used to remove short-term behaviour has a cut-off frequency of  $100\text{ days}^{-1}$ , instead, the filter used to remove long-term behaviour has a cut-off frequency of  $1\text{ days}^{-1}$ .

## 2.4. Comparison with Real Data

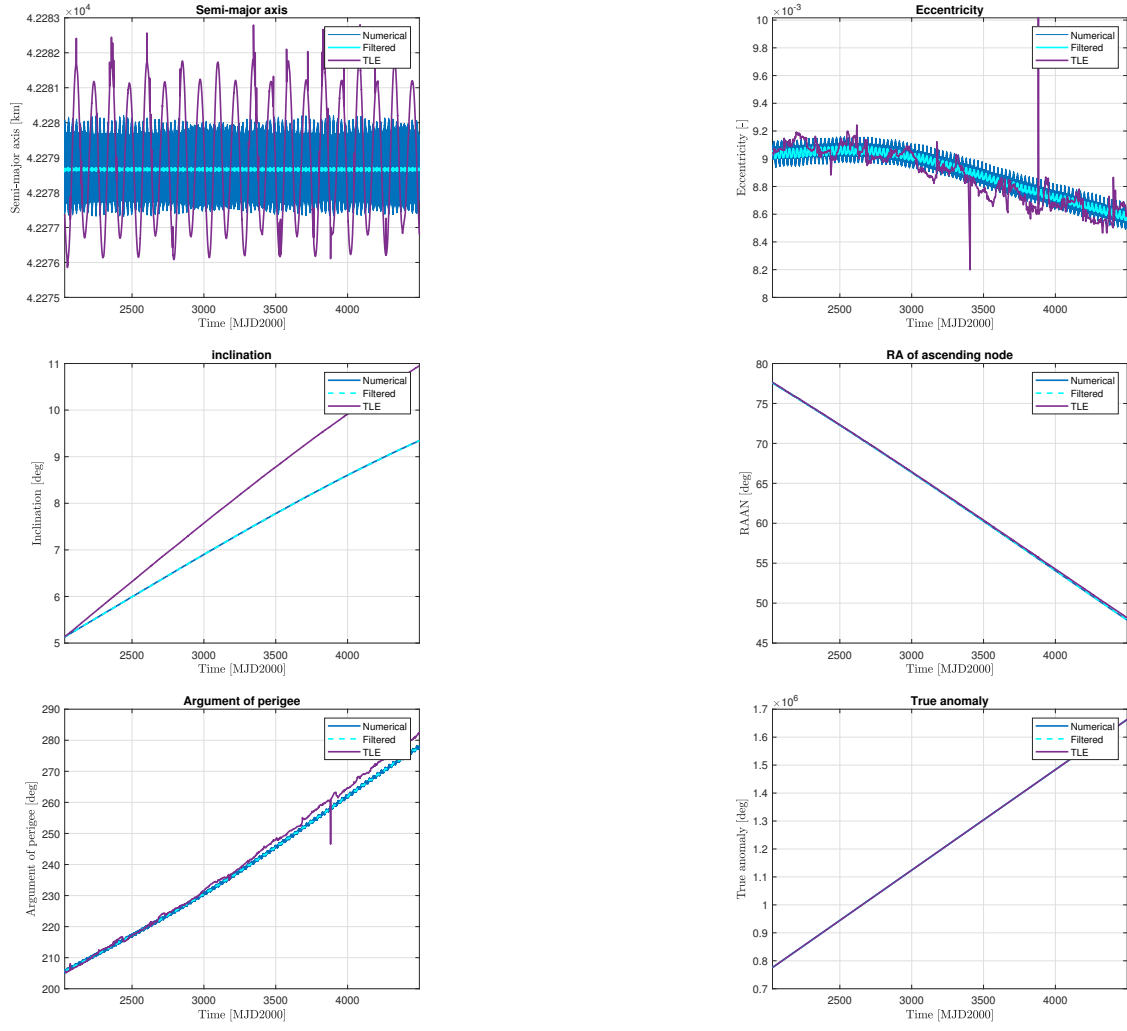


Figure 2.10: Numerical, filtered and TLE data

## Bibliography

- [1] Howard D. Curtis. *Orbital Mechanics for Engineering Students*. Elsevier, 2014.